

# Repurposing Pre-trained Video Diffusion Models for Event-based Video Interpolation

Jingxi Chen<sup>1</sup>, Brandon Y. Feng<sup>2</sup>, Haoming Cai<sup>1</sup>, Tianfu Wang<sup>1</sup>, Levi Burner<sup>1</sup>, Dehao Yuan<sup>1</sup>,  
Cornelia Fermüller<sup>1</sup>, Christopher A. Metzler<sup>1</sup>, Yiannis Aloimonos<sup>1</sup>

<sup>1</sup>University of Maryland, College Park; <sup>2</sup>Massachusetts Institute of Technology

<https://vdm-evfi.github.io/>

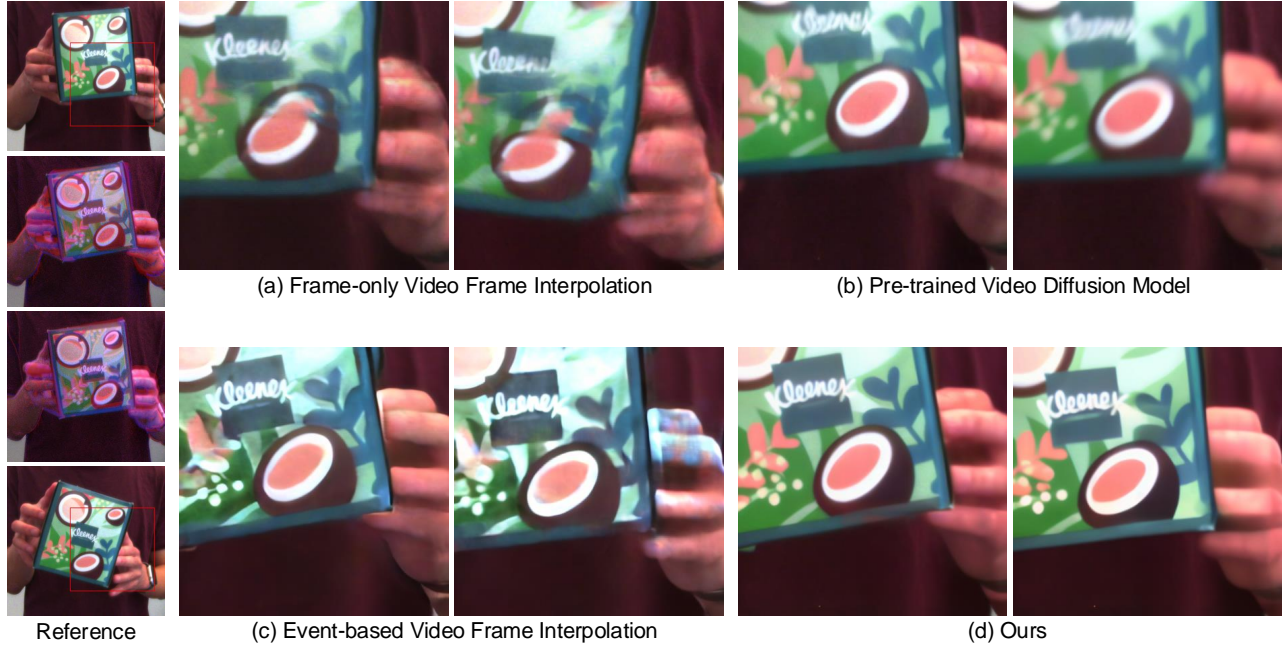


Figure 1. We compare our proposed approach RE-VDM, which adapts a pre-trained video diffusion model for event-based video frame interpolation on unseen real-world data, with three baselines: frame-only interpolation method RIFE [15], test-time optimization of a pre-trained video diffusion model via Time Reversal [10], and event-based interpolation method CBMNet-Large [18], trained on the same dataset as our method. The left-most column shows the start frame, end frame, and reference interpolation frames overlaid with events. Leveraging data priors in the pre-trained video diffusion model and the diffusion process, along with motion guidance controlled by input events, our approach demonstrates superior generalization performance on unseen real-world frames with substantial motion.

## Abstract

Video Frame Interpolation aims to recover realistic missing frames between observed frames, generating a high-frame-rate video from a low-frame-rate video. However, without additional guidance, the large motion between frames makes this problem ill-posed. Event-based Video Frame Interpolation (EVFI) addresses this challenge by using sparse, high-temporal-resolution event measurements as motion guidance. This guidance allows EVFI methods to significantly outperform frame-only methods. However, to date,

EVFI methods have relied on a limited set of paired event-frame training data, severely limiting their performance and generalization capabilities. In this work, we overcome the limited data challenge by adapting pre-trained video diffusion models trained on internet-scale datasets to EVFI. We experimentally validate our approach on real-world EVFI datasets, including a new one that we introduce. Our method outperforms existing methods and generalizes across cameras far better than existing approaches.

## 1. Introduction

Event cameras are a novel class of neuromorphic sensors offering unique advantages, including high dynamic range and high temporal resolution [11]. One significant application of event cameras is Event-based Video Frame Interpolation (EVFI) [18, 23, 36–38, 42]. By capturing traditional frames alongside high temporal resolution events, event data can fill in missing motion information between frames, aiding in interpolation. This approach avoids the ill-posed problem of frame-only interpolation, where large motion between frames introduces excessive degrees of freedom, making the interpolation of frames infeasible.

Current state-of-the-art (SOTA) EVFI methods achieve impressive performance when trained and tested on the same dataset. However, when the test set differs from the training set with changes in data and motion distribution, these methods experience significant performance degradation, as we can see in Fig. 1. This issue arises from two main factors. First, compared to broader fields like video generation, the EVFI field is much smaller, with limited data quantity and quality. Second, the models used in EVFI are highly specialized, with constrained representational power.

Recent advances in generative AI, particularly in video generation, have spurred significant progress in the field. Leading companies have invested substantial resources into building massive, high-quality datasets [8] and developing foundation models for video generation [8, 14]. Most of these foundation models are video diffusion models. By leveraging millions of high-quality commercial video clips and billions of parameters, these diffusion models achieve impressive generalization performance compared to previous approaches. A comparison between video generation and EVFI fields is presented in Table 1. The primary differences between these fields lie in dataset quality/size and model parameter scale, the EVFI field lacks the extensive commercial datasets and large model sizes found in video generation, impacting its models’ generalization and representational power.

This raises a natural question: *Can we adapt pre-trained video diffusion foundation models for EVFI to leverage their learned data priors and model design advantages?*

In this work, we introduce the first approach, RE-VDM, for adapting pre-trained video diffusion foundation models to the EVFI task, aiming to bridge EVFI with generative AI by leveraging robust data priors and foundation models. To achieve this, we address key technical challenges. First, for data-efficient adaptation, we train an additional subset of the model with event-based control on small EVFI datasets inspired by [40], while keeping the original weights frozen to avoid catastrophic forgetting of learned data priors as explained in Section 3.2. Second, while video generation aims to produce diverse videos without strict realism constraints, EVFI requires ground-truth fidelity to accurately

| Feature                                   | Video Generation                    | EVFI          |
|---|-------------------------------------|---------------|
| Dataset Size [7, 20, 29]                  | $10^7$                              | $10^2$        |
| Dataset Quality [7, 18, 20, 29, 35, 38]   | Commercial                          | Custom        |
| Model Type [7, 18, 23, 36, 38]            | Video Diffusion (Foundation) Models | Custom Models |
| Model Size [7, 18, 23, 29, 36, 38]        | $10^{10}$                           | $10^8$        |
| Video Generation Type [7, 18, 23, 36, 38] | Extrapolation                       | Interpolation |

Table 1. Comparison between video generation and event-based video frame interpolation (EVFI) fields reveals major differences in dataset size, quality, and model design. Video generation datasets are orders of magnitude larger than EVFI datasets and are of commercial-level quality. Models for video generation are typically foundation models with billions of parameters. With abundant training data and large-scale foundation models, video diffusion models are well-suited for generalized video generation tasks.

recover missing frames. To preserve motion and appearance fidelity, we employ upsampling and Per-tile Denoising and Fusion as explained in Section 3.4 as the test-time optimization for video generation with high-fidelity appearance and event-based motion control. Finally, unlike video generation, which is an extrapolation task based on an image or text prompt, EVFI requires interpolation between the start and end frames. To address this, we develop a test-time optimization approach that generates event-based video latents from both the start and end frames at each denoising step, fusing them for a consistent, interpolated result that incorporates information from both frames, as explained in Section 3.5

For a robust evaluation, we compare the generalization performance of our approach against representative frame-only, event-based, and pre-trained video diffusion models for frame interpolation across multiple datasets, including self-collected Clear-Motion test sequences. The results demonstrate the potential and advantages of this adaptation. We also discuss the limitations observed, highlighting the exploratory nature of our work. To summarize, our contributions are

- We present the first approach for adapting pre-trained video diffusion foundation models to the Event-based Video Frame Interpolation task, leveraging the strong data priors learned from large video generation datasets and the inherent advantages of video diffusion models.
- Experimental results demonstrate the strong potential of the adapted video diffusion model for the EVFI task, showing excellent generalization on unseen real-world data and consistency in reconstructed frames.

## 2. Related Work

### 2.1. Event Camera and Video Frame Interpolation

Event cameras are neuromorphic sensors that capture the brightness changes in the scene, and the brightness changes are primarily due to the camera’s motion and object motion in the scene. For this reason, events captured by event cameras can be used to compute motion-related information, for example, optical flow, motion segmentation, and

ego-motion [3–6, 24, 25, 27, 44, 45]. Various methods have been proposed to reconstruct intensity videos from event streams alone, demonstrating that while feasible, the quality of such reconstructions is significantly limited by camera and object motion [9, 30]. Combining events with images extends beyond event-only applications, offering powerful capabilities for tasks like image deblurring and video frame interpolation [36–38, 42]. This approach leverages events as cues to bridge the gap between frames, thus avoiding the ill-posed challenges faced by frame-only methods [1, 15, 17, 19, 21, 28] when interpolating between frames with substantial motion.

## 2.2. Diffusion and Video Diffusion Models

Diffusion models [13, 34] is an emerging class of image generative models that model the reverse diffusion process of recovering data from noise. Starting from data  $\mathbf{x}_0$  from the data distribution  $p_{data}(\mathbf{x})$ , The diffusion model tries to reverse the forward diffusion process as an  $N$  step Markov chain  $\{\mathbf{x}_i\}, i \in [0, N]$  that satisfies the marginal distribution

$$p_{\alpha_i}(\mathbf{x}_i | \mathbf{x}_0) = \mathcal{N}(\mathbf{x}_i; \alpha(t)\mathbf{x}_0, \sigma(t)^2 \mathbf{I}). \quad (1)$$

Here,  $\alpha(t), \sigma(t)$  represents a noise schedule. Diffusion models have demonstrated remarkable image generation quality and diversity. Stable Diffusion [31] shifts the generation process to a low-dimensional latent space, greatly reducing computational cost. Trained on massive online text-image pair datasets [33], Stable Diffusion exhibits strong image generation capabilities.

Video diffusion models [8, 14] add temporal layers on top of existing image diffusion models to jointly denoise multiple consistent image frames. Stable Diffusion Video (SVD) [8] is built on top of latent diffusion model and trained on massive video datasets, serving as a strong foundational model for video generation tasks.

## 2.3. Controllable Diffusion Generation Through Fine-Tuning

There have been numerous works on generation conditioned on additional user inputs or control [31, 32, 40]. Stable Diffusion [31] uses cross-attention layers in the diffusion U-Net to inject text control. Dreambooth [32] showed that a diffusion model can be fine-tuned for conditional control. ControlNet [40] modifies a trainable copy of the original diffusion U-Net for conditional control. In addition to fine-tuning diffusion models for added controllability, various training-free methods have been proposed to alter the sampling process of image and video diffusion models for more flexible and generalized content synthesis [2, 10, 22, 43]. Latent diffusion models have limitations on generating a limited set of resolutions in a downsampled latent space. MultiDiffusion [2] provides a solution for resolution-agnostic generation by tile-based denoising. When combined with

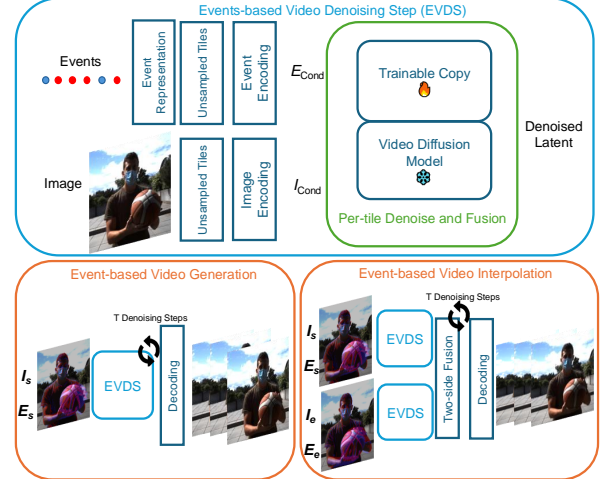


Figure 2. The overview of our proposed approach RE-VDM: for adapting pre-trained video diffusion models includes two tasks: event-based video generation and interpolation. For video generation, the method utilizes the start frame  $I_s$  and forward-time events  $E_s$ . For interpolation, it incorporates both the start frame  $I_s$  and forward-time events  $E_s$ , as well as the end frame  $I_e$  and backward-time events  $E_e$  to achieve consistent results. Unlike video generation, for interpolation, a denoising step  $t$  concludes with Two-side Fusion instead of EVDS.

conditional control, MultiDiffusion has shown to be effective in generating synthetic detailed images under the condition of fine-grained condition control [16]. On the video generation side, [10] proposes a test-time sampling method that empowers video diffusion models to control camera and object motion. [43] enables consistent long-frame generation outside of the trained frame length of a video diffusion model, through simultaneously generating multiple video sequences, and fusing intermediate denoising results of overlapping frames.

## 3. Proposed Approach

### 3.1. Pipeline Overview

Figure 2 presents an overview of our pipeline RE-VDM, for adapting pre-trained video diffusion models to event-based video generation and interpolation tasks. The key difference is that interpolation applies our EVDS on both the start frame  $I_s$  for forward-time video denoising/generation and the end frame  $I_e$  for backward-time video denoising/generation. At each denoising step, forward-backward consistency is enforced to achieve accurate interpolation. Details and design of each key component are explained in the following subsections.

In this work, without loss of generality, we assume that the pre-trained video diffusion model used is a Latent Diffusion Model, as is common in most video diffusion models.

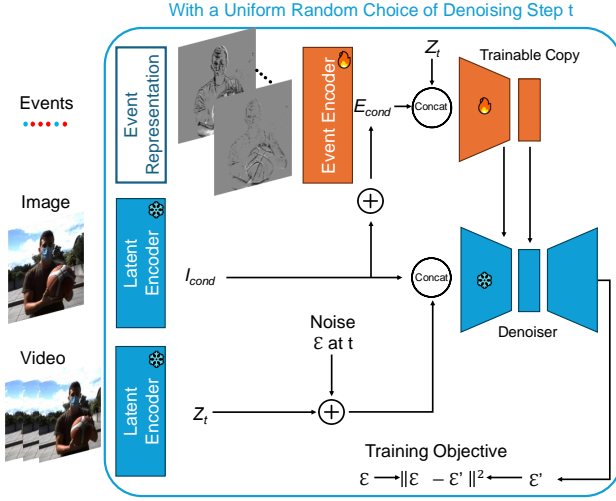


Figure 3. The illustration depicts our training scheme for adapting a pre-trained video diffusion model to event-based video denoising. Our approach uses a frozen denoiser network from the pre-trained model, augmented with a trainable subset of blocks copied from the frozen denoiser.

### 3.2. Data-Efficient Adaptation of Pre-trained Video Diffusion Models

In this section we will explain the details for introducing the additional event-based motion control to pre-trained video diffusion models. As discussed in Section 1 and shown in Table 1, the large training datasets and model size of pre-trained video diffusion foundation models provide impressive generalization power for video generation tasks. However, these factors also limit the fine-tuning flexibility of the pre-trained model weights on existing EVFI datasets due to the risk of catastrophic forgetting, stemming from significant differences in data size and quality.

To prevent catastrophic forgetting of the learned data priors in pre-trained video diffusion foundation models, we drew inspiration from the [40] approach for controllable image diffusion models, known for its impressive performance with small data adaptation. In our design, we keep the original weights of the video diffusion models frozen during training. Event-based control is introduced by training only a subset of blocks, copied from the original denoiser network, to serve as additional residuals to corresponding block outputs in the frozen denoiser network. A detailed illustration is provided in Figure 3.

The added event encoder and trainable copy aim to learn the correct encoding for events as the control condition,  $E_{cond}$ , as well as the block output residuals for the frozen pre-trained denoiser network by optimizing the trainable copy. We use the standard diffusion objective, which minimizes the mean squared error loss between the predicted noise  $\epsilon'$  and the ground truth noise  $\epsilon$  added to the video latent

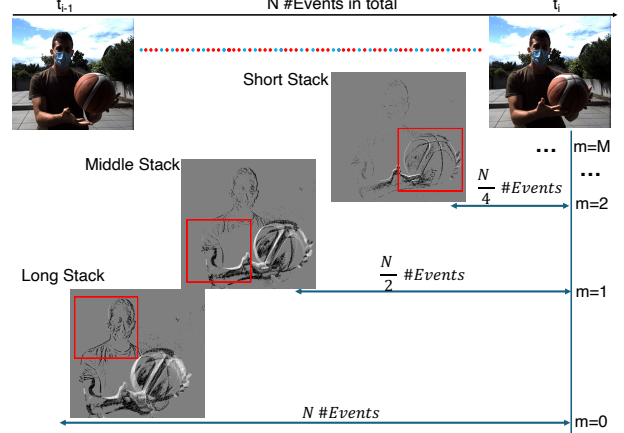


Figure 4. Our multi-stack event representation is illustrated as follows. The stack begins from the target frame at  $t_i$  and expands backward in time to the previous frame  $t_{i-1}$ . Within each stack, the number of events accumulated from  $t_i$  is halved from the previous stack. In the long stack ( $m = 0$ ), the slowest-moving objects, such as around the human head, appear sharp; in the middle stack ( $m = 1$ ), slower-moving objects, like the human arm, are clear; and in the short stack ( $m = 2$ ), the fastest-moving objects, such as the ball, are sharp. This approach ensures that the event data provides adequate control information for generating frame  $t_i$ .

for a uniformly randomly sampled denoising time  $t$ .

During inference, the only difference from the training scheme is the absence of a given video latent  $Z_t$  and noise  $\epsilon$  for a sampled denoising time  $t$ . Instead, the initial noisy latent  $Z_T$  is generated from standard Gaussian noise  $N(0, 1)$  at the beginning of the denoising process.

### 3.3. Events as the Control Condition

To introduce events as the control condition for the video generation process, we incorporate two main components: 1) Event Representation and 2) Event Encoder. For event representation, we adopt a multi-stack approach, inspired by [26], which captures both fast- and slow-moving objects within a multi-channel, frame-like format. An example of this multi-stack event representation is illustrated in Figure 4. Based on this representation, our event encoder consists of a series of convolutional layers with stride to downsample the input event representation into the event latent  $E_{cond}$ , matching the dimension of the image latent  $I_{cond}$ .

### 3.4. Per-tile Denoising and Fusion

Due to the substantial memory demands of training and generating high-resolution video, most existing video diffusion models, such as Stable Video Diffusion (SVD) [7], are Latent Diffusion Models, meaning they operate in the latent space with downsampled spatial resolution rather than in the original pixel space. As illustrated in Figure 3, for an input RGB image/video of shape  $[B, F, 3, H, W]$ , where  $B$  is



Figure 5. The VAE encoding/decoding loss of small details in the original input image. In (a), we show the original image, sized 970 x 625. In (b), we pad the image to the nearest multiple of 8, then encode and decode it back. After decoding, the PSNR drops to 21.50, with noticeable detail loss in the zoomed-in view. In (c), we pad to the nearest multiple of 8, upsample to twice the original width and height, then encode and decode. After decoding, the PSNR increases to around 24.92, with no significant loss of details in the zoomed-in view.

the batch size,  $F$  is the number of frames,  $W$  is the width, and  $H$  is the height, a latent encoder ( $\mathcal{E}$ ) and decoder ( $\mathcal{D}$ ), typically based on a Variational Autoencoder (VAE), convert the input into image latents of shape  $[B, F, C_{latent}, \frac{H}{d}, \frac{W}{d}]$  and decode it back. Here,  $d$  is the downsample factor, set to 8 in SVD, and  $C_{latent}$  is the number of latent channels, set to 4 in SVD.

The Latent VAE encoder/decoder approach is effective for video generation, where realism is less critical, as the task often involves stylized animation rather than high-detail photorealism. However, for EVFI, minimizing the loss from downsampled encoding/decoding is essential, as our goal is to recover realistic missing frames between keyframes. A key observation is that small details can be lost after VAE encoding/decoding. Upsampling the input mitigates this loss, as shown in Figure 5, where increasing input upsampling effectively reduces encoding/decoding loss on fine details.

Additionally, as illustrated in Figure 3, spatial downampling of the input image to create image latents can also reduce event control accuracy, since the trainable copy’s input consists of combined image latents  $I_{cond}$  and event latents  $E_{cond}$  of the same dimensions. However, upsampling input videos substantially increases computational costs for both training and testing. To address this, we divide the upsampled input video into overlapping cropped tiles of fixed width and height, applying EVDS to each tile independently. We then fuse the denoised latents of tiles to achieve consistent latents for each image and video, preserving shared

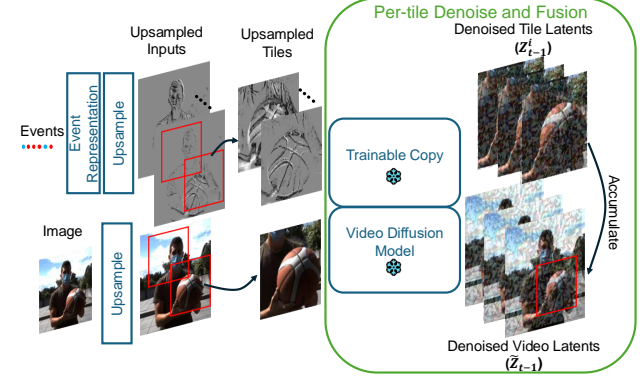


Figure 6. The Per-tile Denoising and Fusion process is a test-time optimization applied during inference to enhance the fidelity of video generation appearance and improve event-based motion control accuracy. During each denoising step, our model operates on upsampled tiles of the input image and event representations to predict denoised latents for each tile  $i$  at a denoising time  $t$  ( $Z_{t-1}^i$ ). These denoised tile latents are then accumulated to obtain the predicted denoised latents for the entire video ( $\tilde{Z}_{t-1}$ ) at that denoising step  $t$ .

context across overlapping regions

Our Per-tile Denoising and Fusion process is illustrated in Figure 6. We employ tiled diffusion [2] by first dividing the latent canvas into  $n$  overlapping tiles. For the denoised tile latents at tile  $i$  at denoising step  $t$ , we use an accumulation process to fuse them into the denoised latent for the entire upsampled video. The accumulation process takes in  $n$  tile latents and outputs the fused latent:

$$\tilde{Z}_{t-1} = \sum_{i=1}^n \frac{W_i}{\sum_{j=1}^n W_j} \otimes Z_{t-1}^i, \quad (2)$$

where  $\tilde{Z}_{t-1} \in \mathbb{R}^{F \times H \times W \times d}$ , with  $F$  representing the number of frames,  $H$  and  $W$  the height and width of the upsampled latent canvas, and  $d$  the latent dimension.  $Z_{t-1}^i$  contains the denoised latents of the  $i$ -th grid tile,  $Z_{t-1}^i \in \mathbb{R}^{F \times h \times w \times d}$ , where  $h$  and  $w$  denote the height and width of each latent tile.  $W_i \in \mathbb{R}^{F \times h \times w}$  represents pixel-wise weights for the  $i$ -th tile. In our implementation, we assign equal weights, averaging the denoised latents across overlapping tiles.

### 3.5. From Video Generation to Frame Interpolation

Our approach thus far is designed to generate realistic video controlled by events from the start frame, suited for event-based video generation (extrapolation). However, the EVFI task requires frame interpolation, which involves utilizing information from both the start and end frames.

The most straightforward approach to achieve frame interpolation would be to fine-tune base video diffusion models to accept an additional channel for the second image. However, as previously discussed, fine-tuning pre-trained video

| Method             | Category                              | BS-ERGB (3 skips) |                 |                    | HQF (3 skips)   |                 |                    | Clear-Motion (15 skips) |                 |                    |
|--------------------|---------------------------------------|-------------------|-----------------|--------------------|-----------------|-----------------|--------------------|-------------------------|-----------------|--------------------|
|                    |                                       | PSNR $\uparrow$   | SSIM $\uparrow$ | LPIPS $\downarrow$ | PSNR $\uparrow$ | SSIM $\uparrow$ | LPIPS $\downarrow$ | PSNR $\uparrow$         | SSIM $\uparrow$ | LPIPS $\downarrow$ |
| Time Reversal [10] | Pre-trained Video Diffusion           | 17.86             | 0.59            | 0.27               | 17.92           | 0.53            | 0.18               | 13.71                   | 0.70            | 0.44               |
| RIFE [15]          | Frame-only Video Frame Interpolation  | 23.30             | 0.83            | 0.09               | 25.34           | 0.76            | 0.05               | 16.93                   | 0.76            | 0.35               |
| CBMNet-Large [18]  | Event-based Video Frame Interpolation | 26.24             | 0.79            | 0.22               | 28.73           | 0.84            | 0.09               | 22.26                   | 0.86            | 0.39               |
| RE-VDM (Ours)      | Adapted Video Diffusion               | <b>27.74</b>      | <b>0.88</b>     | <b>0.12</b>        | <b>29.04</b>    | <b>0.89</b>     | <b>0.06</b>        | <b>22.94</b>            | <b>0.88</b>     | <b>0.37</b>        |

Table 2. We compare our method on real-world EVFI datasets against representative and SOTA methods, including the pre-trained video diffusion model (Time Reversal), frame-only method (RIFE), and event-based video frame interpolation method (CBMNet-Large). For CBMNet-Large, we use publicly available model checkpoints trained on the same BS-ERGB dataset as our approach. For the BS-ERGB and HQF datasets, we use a skip number of 3 as in the EVFI papers, we evaluate all interpolated frames. For our Clear-Motion test sequences, we use a skip number of 15 for evaluation on large motion scenarios, we evaluate the 4th, 8th, and 12th interpolated frames. To control for VAE encoding/decoding loss, as discussed in Section 4.2, we apply VAE encoding/decoding to all model outputs.

diffusion foundation models on the EVFI dataset risks catastrophic forgetting of the learned data priors, undermining the purpose of adaptation.

To address this, we opted for a test-time optimization approach that avoids further training, enabling our video generation model to perform EVFI. As shown in Figure 2, inspired by [10], our key idea is to run the EVDS at each denoising step from both the start frame  $I_s$  and the end frame  $I_e$ , producing two sets of predicted denoised video latents. We then apply a Two-side Fusion of these denoised latents to obtain consistent results. This approach allows us to achieve frame interpolation, effectively leveraging information from both frames. The details of the Two-Side Fusion algorithm are as follows: For a denoising time  $t$ , the forward denoised video latents from the start frame  $I_s$  and forward-time events  $E_s$  are  $Z_{t-1}^s = EVDS(I_s, E_s)$ , and the backward denoised video latents from the end frame  $I_e$  and backward-time events are  $Z_{t-1}^e = EVDS(I_e, E_e)$ , with  $Z_{t-1}^s, Z_{t-1}^e \in \mathbb{R}^{F \times H \times W \times d}$ . To make the final denoised video latent  $\tilde{Z}_{t-1}$  consistent with information from both the start and end frames, we assign linearly increasing weights,  $W_f \in \mathbb{R}^F$ , where  $W_0 = 0$  and  $W_1 = 1$ . This allows us to fuse the final video latents  $\tilde{Z}_{t-1}$  as follows:

$$\tilde{Z}_{t-1} = W_f \otimes Z_{t-1}^s + (1 - W_f) \otimes \text{flip}(Z_{t-1}^e) \quad (3)$$

where  $\text{flip}$  denotes reversing the temporal order of the frames in  $Z_{t-1}^e$ . The intuition behind this approach is that frames near the start frame rely more heavily on information from the start frame and forward-time events, while frames near the end rely more on the end frame and backward-time events, in the middle, they balance information from both.

## 4. Experimental Results

### 4.1. Datasets and Training Details

To robustly evaluate the generalized frame interpolation performance of our approach, we select several real-world event camera datasets. The BS-ERGB dataset [37], the most cited

for EVFI, provides aligned RGB and event video with large motion between frames, mainly featuring static cameras capturing dynamic objects. The HQF dataset [35] includes grayscale video aligned with events, with more sequences involving a moving event camera.

In addition to existing datasets, we include our self-collected Clear-Motion test sequences, which provide aligned RGB frames and events, capturing previously unseen large, distinct object motions between frames. This addition expands the range of scenarios covered beyond existing datasets, with details provided in the Supplementary Material.

The pre-trained video diffusion model we used is Stable Video Diffusion [7] for 14-frame image-to-video generation. We trained our model with an effective batch size of 64, using a batch size of 4 per GPU and a gradient accumulation factor of 16. Training was conducted solely on the BS-ERGB dataset, and the model was tested on other unseen datasets without fine-tuning. All training was performed on 4 NVIDIA RTX A6000 GPUs, each with 50GB of memory.

### 4.2. Evaluation Strategy

To evaluate generalized frame interpolation performance, we compare our approach with representative methods from three categories: frame-only interpolation (RIFE [15]), test-time optimization of pre-trained diffusion models (Time Reversal [10]), and event-based interpolation (CBMNet [18]). We use publicly available CBMNet checkpoints trained on the BS-ERGB dataset for evaluation. For Per-tile Denoising and Fusion in our method, which uses upsampled tiles to reduce detail loss and enhance event control accuracy, we apply an upsample factor of 2 for the BS-ERGB and Clear-Motion datasets and 3 for the HQF dataset.

For evaluation metrics, we use average frame PSNR [12], SSIM [39], and LPIPS [41] for the interpolated frames. Since SVD is a latent diffusion model that uses a VAE to encode and decode between latent and pixel space, we apply VAE encoding and decoding to all model outputs. This eliminates the impact of discrepancies between the VAE-decoded frame distribution and the ground truth frame distribution,

accounting for differences in noise patterns, small details, and tone mapping.

### 4.3. Evaluation on Video Frame Interpolation

In this section, we present both qualitative and quantitative results that demonstrate the generalized performance of our proposed method compared to representative and SOTA methods for video frame interpolation, as shown in Table 2. As seen in the table, both Time Reversal and RIFE struggle with real-world video frame interpolation, as these methods do not utilize events between frames. Without event data, large or irregular motion between frames introduces too many degrees of freedom, making the interpolation problem ill-posed. In contrast, the SOTA event-based interpolation method, CBMNet-Large, can handle large motions by leveraging cues from events, similar to our approach. However, its performance on both the test set from the training dataset and unseen datasets is consistently lower than ours across all metrics. This difference is due to two factors: 1) as discussed in Section 1 and Table 1, the pre-trained video diffusion foundation model in our approach offers a superior data prior from its extensive training on large video generation datasets, and 2) our model’s backbone, a highly representative pre-trained video diffusion model, provides advantages over custom models typically used in EVFI.

The effectiveness of our approach on real-world, unseen data for video frame interpolation is clearly demonstrated in the qualitative comparisons in Figures 7, 8, 9, 10 and 11. Due to the ill-posed nature of interpolating frames with large motion, frame-only methods like RIFE and Time Reversal struggle to accurately reconstruct object locations and appearances. Notably, although Time Reversal’s reconstructions are not ideal, they show relatively higher temporal consistency compared to RIFE and CBMNet-Large. This highlights the strong data prior and temporal consistency advantage of pre-trained video diffusion foundation models, as discussed in Table 1. This observation supports our motivation to adapt these models for the EVFI task.

While CBMNet-Large uses event data to guide interpolation and achieves similar object and texture placements, it lacks generalization on unseen object and camera motion compared to our method, as shown in Figures 7, 8, 9, 10, despite being trained on the same dataset. Additionally, CBMNet-Large suffers from frame-to-frame inconsistencies due to its frame-by-frame inference design, evident in Figure 11. CBMNet-Large produces frames with inconsistent textures and shapes on the ball and hand, whereas our method accurately reconstructs the challenging, regular shapes of both. This advantage is due to the strong data priors and foundational design of the pre-trained video diffusion model, allowing for consistent reconstruction across frames. Unlike CBMNet-Large, video diffusion models process multiple frames cohesively. These results underscore the effective-

ness of our adaptation for generalized EVFI on real-world, unseen data and highlight the advantage of video diffusion models in achieving consistency across video frames.

### 5. Limitations

Despite the promising results, adapting pre-trained video diffusion models to the EVFI task presents several limitations. First, the pre-trained VAE encoder and decoder, used for conversion between pixel space and latent space, have limited representational power, often resulting in color shifts and loss of small details. Second, the adapted video diffusion model tends to smooth out certain regions, likely due to its difficulty in preserving fine textures within the downsampled latent space or the need for a prohibitively high upsampling factor to prevent smoothing.

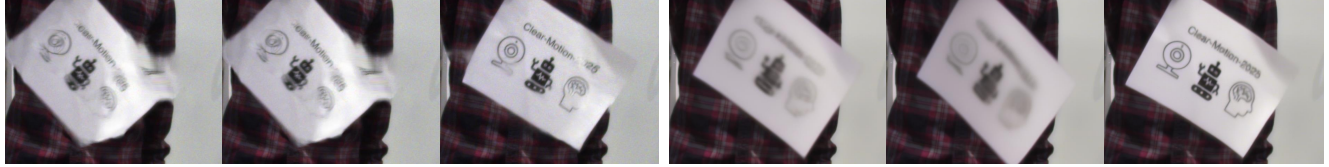
These limitations stem from the current state of pre-trained video diffusion foundation models. However, as the field of video generation evolves rapidly, we anticipate that many of these issues could be mitigated or resolved with newer, more advanced pre-trained models in the near future.

### 6. Conclusion

In this work, we explore, for the first time, the adaptation of pre-trained video diffusion foundation models for the event-based video frame interpolation (EVFI) task, as a foundational step toward integrating event camera technology with the era of Generative AI. We present an approach to address the key challenges in adapting video diffusion models to EVFI. We use data-efficient adaptation to bridge the gap in data quality and size between large-scale video generation datasets and smaller EVFI datasets, minimizing the risk of catastrophic forgetting. Our method also includes test-time optimization techniques: Per-tile Denoising and Fusion to reduce encoding/decoding losses between pixel and latent spaces, preserving high-fidelity appearance and accurate event-based motion control, and Two-side Fusion, which incorporates both start and end frame information at each denoising step for improved interpolation consistency. We also discuss current limitations in pre-trained video diffusion models for EVFI. Lastly, we demonstrate our model’s superior generalization and frame consistency on unseen real-world data, highlighting the motivation and potential of our approach.



(a) Illustration of start frame, end frame and events in-between overlaid with reference frames



(b) RIFE

(c) Time Reversal



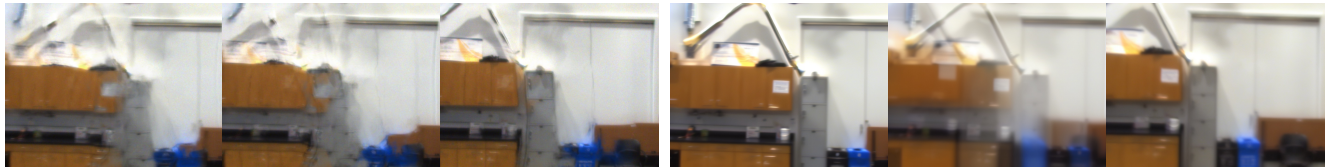
(d) CBMNet-Large

(e) Ours

Figure 7. An illustration showcasing the qualitative comparison on the Clear-Motion sequence Paper\_Waving, which involves waving a paper with simple texture, with 11 skips between the start and end frames. We present the interpolated 4th, 7th, and 10th frames. (Zoom in for the best viewing experience)

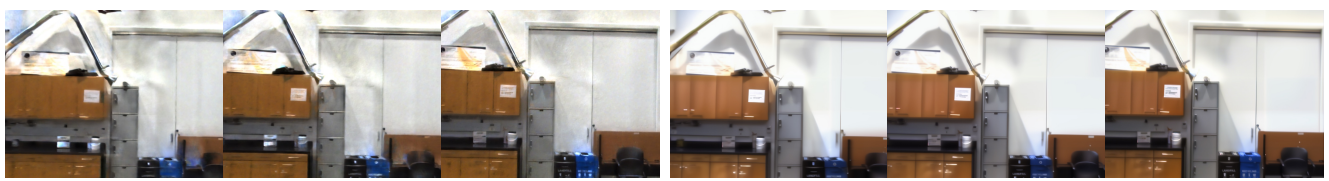


(a) Illustration of start frame, end frame and events in-between overlaid with reference frames



(b) RIFE

(c) Time Reversal



(d) CBMNet-Large

(e) Ours

Figure 8. An illustration showcasing the qualitative comparison on the Clear-Motion sequence Camera\_Far, which involves large camera motion capturing nearby objects, with 11 skips between the start and end frames. We present the interpolated 4th, 7th, and 10th frames. (Zoom in for the best viewing experience)

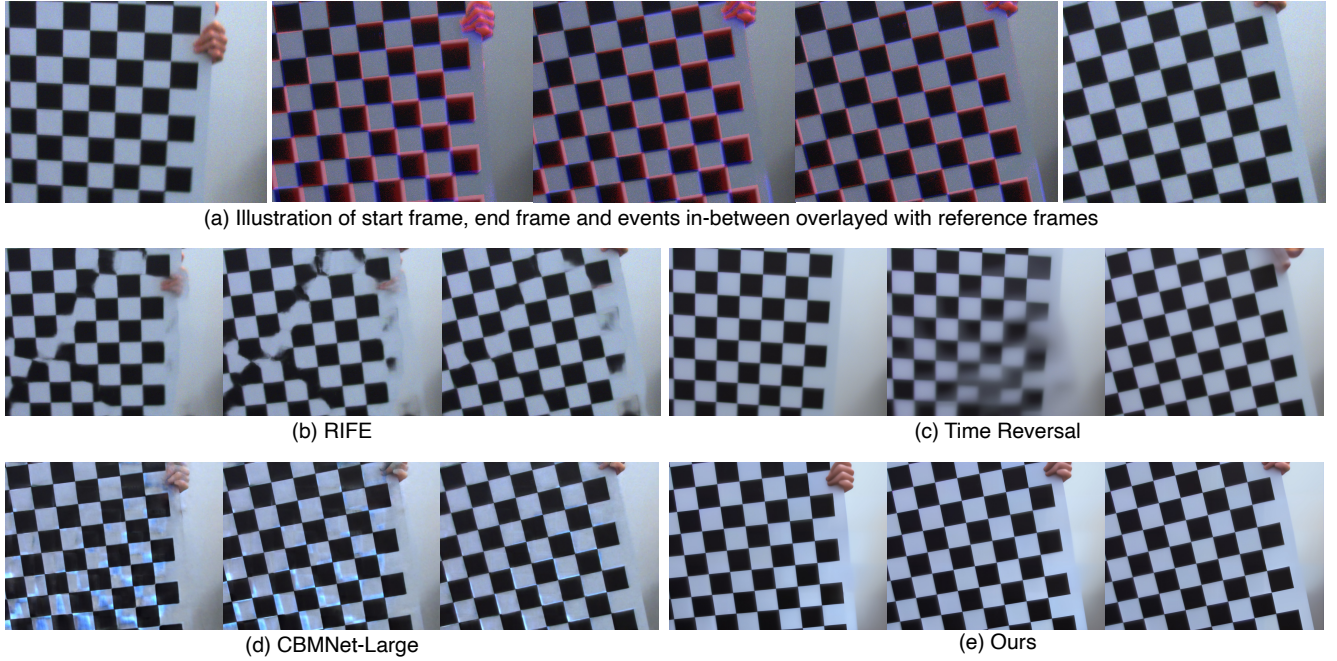


Figure 9. An illustration showcasing the qualitative comparison on the Clear-Motion sequence Checkerboard\_Planar, which involves large planar motion of a nearby checkerboard, with 11 skips between the start and end frames. We present the interpolated 4th, 7th, and 10th frames. (Zoom in for the best viewing experience)



Figure 10. An illustration showcasing the qualitative comparison on the HQF dataset for the sequence poster\_pillar\_1, involving moving cameras capturing nearby posters, with 3 skips between the start and end frames. All interpolated frames are presented. (Zoom in for the best viewing experience)



Figure 11. The qualitative visualization of our experimental results on the BS-ERGB test sequences, with 3 skips between the start and end frames. All interpolated frames are presented. This sequence features fast motion of a hand and a rising, spinning ball, shows that our method is the only approach capable of maintaining the regular texture shapes on both the ball and hand across the interpolated frames in this challenging scenario. **Please refer to the website for additional results on datasets and videos, the videos provide further and straightforward comparisons of reconstruction consistency.**

## References

- [1] Wenbo Bao, Wei-Sheng Lai, Chao Ma, Xiaoyun Zhang, Zhiyong Gao, and Ming-Hsuan Yang. Depth-aware video frame interpolation. In *Proceedings of the IEEE/CVF conference on computer vision and pattern recognition*, pages 3703–3712, 2019. [3](#)
- [2] Omer Bar-Tal, Lior Yariv, Yaron Lipman, and Tali Dekel. Multidiffusion: Fusing diffusion paths for controlled image generation. In *ICML*. PMLR, 2023. [3](#), [5](#)
- [3] Patrick Bardow, Andrew J Davison, and Stefan Leutenegger. Simultaneous optical flow and intensity estimation from an event camera. In *Proceedings of the IEEE conference on computer vision and pattern recognition*, pages 884–892, 2016. [3](#)
- [4] Francisco Barranco, Cornelia Fermüller, and Yiannis Aloimonos. Contour motion estimation for asynchronous event-driven cameras. *Proceedings of the IEEE*, 102(10):1537–1556, 2014.
- [5] Francisco Barranco, Cornelia Fermüller, and Eduardo Ros. Real-time clustering and multi-target tracking using event-based sensors. In *2018 IEEE/RSJ International Conference on Intelligent Robots and Systems (IROS)*, pages 5764–5769. IEEE, 2018.
- [6] Ryad Benosman, Sio-Hoi Ieng, Charles Clercq, Chiara Bar-  
tolazzi, and Mandyam Srinivasan. Asynchronous frameless event-based optical flow. *Neural Networks*, 27:32–37, 2012. [3](#)
- [7] Andreas Blattmann, Tim Dockhorn, Sumith Kulal, Daniel Mendelevitch, Maciej Kilian, Dominik Lorenz, Yam Levi, Zion English, Vikram Voleti, Adam Letts, et al. Stable video diffusion: Scaling latent video diffusion models to large datasets. *arXiv preprint arXiv:2311.15127*, 2023. [2](#), [4](#), [6](#)
- [8] Andreas Blattmann, Robin Rombach, Huan Ling, Tim Dockhorn, Seung Wook Kim, Sanja Fidler, and Karsten Kreis. Align your latents: High-resolution video synthesis with latent diffusion models. In *CVPR*, 2023. [2](#), [3](#)
- [9] Pablo Rodrigo Gantier Cadena, Yeqiang Qian, Chunxiang Wang, and Ming Yang. Sparse-e2vid: A sparse convolutional model for event-based video reconstruction trained with real event noise. In *Proceedings of the IEEE/CVF Conference on Computer Vision and Pattern Recognition*, pages 4149–4157, 2023. [3](#)
- [10] Haiwen Feng, Zheng Ding, Zhihao Xia, Simon Niklaus, Victoria Abrevaya, Michael J Black, and Xuaner Zhang. Explorative inbetweening of time and space. In *ECCV*, 2025. [1](#), [3](#), [6](#)
- [11] Guillermo Gallego, Tobi Delbrück, Garrick Orchard, Chiara

Bartolozzi, Brian Taba, Andrea Censi, Stefan Leutenegger, Andrew J Davison, Jörg Conradt, Kostas Daniilidis, et al. Event-based vision: A survey. *IEEE transactions on pattern analysis and machine intelligence*, 44(1):154–180, 2020. 2

[12] Rafael C Gonzalez. *Digital image processing*. Pearson education india, 2009. 6

[13] Jonathan Ho, Ajay Jain, and Pieter Abbeel. Denoising diffusion probabilistic models. In *NeurIPS*, 2020. 3

[14] Jonathan Ho, Tim Salimans, Alexey Gritsenko, William Chan, Mohammad Norouzi, and David J Fleet. Video diffusion models. 2022. 2, 3

[15] Zhewei Huang, Tianyuan Zhang, Wen Heng, Boxin Shi, and Shuchang Zhou. Real-time intermediate flow estimation for video frame interpolation. In *European Conference on Computer Vision*, pages 624–642. Springer, 2022. 1, 3, 6

[16] Yuru Jia, Lukas Hoyer, Shengyu Huang, Tianfu Wang, Luc Van Gool, Konrad Schindler, and Anton Obukhov. Dginstyle: Domain-generalizable semantic segmentation with image diffusion models and stylized semantic control. In *ECCV*, 2025. 3

[17] Huaizu Jiang, Deqing Sun, Varun Jampani, Ming-Hsuan Yang, Erik Learned-Miller, and Jan Kautz. Super slomo: High quality estimation of multiple intermediate frames for video interpolation. In *Proceedings of the IEEE conference on computer vision and pattern recognition*, pages 9000–9008, 2018. 3

[18] Taewoo Kim, Yujeong Chae, Hyun-Kurl Jang, and Kuk-Jin Yoon. Event-based video frame interpolation with cross-modal asymmetric bidirectional motion fields. In *Proceedings of the IEEE/CVF Conference on Computer Vision and Pattern Recognition (CVPR)*, pages 18032–18042, 2023. 1, 2, 6

[19] Lintong Kong, Boyuan Jiang, Donghao Luo, Wenqing Chu, Xiaoming Huang, Ying Tai, Chengjie Wang, and Jie Yang. Ifrnet: Intermediate feature refine network for efficient frame interpolation. In *Proceedings of the IEEE/CVF Conference on Computer Vision and Pattern Recognition*, pages 1969–1978, 2022. 3

[20] Yixin Liu, Kai Zhang, Yuan Li, Zhiling Yan, Chujie Gao, Ruoxi Chen, Zhengqing Yuan, Yue Huang, Hanchi Sun, Jianfeng Gao, et al. Sora: A review on background, technology, limitations, and opportunities of large vision models. *arXiv preprint arXiv:2402.17177*, 2024. 2

[21] Liying Lu, Ruizheng Wu, Huajia Lin, Jiangbo Lu, and Jiaya Jia. Video frame interpolation with transformer. In *Proceedings of the IEEE/CVF Conference on Computer Vision and Pattern Recognition*, pages 3532–3542, 2022. 3

[22] Andreas Lugmayr, Martin Danelljan, Andres Romero, Fisher Yu, Radu Timofte, and Luc Van Gool. Repaint: Inpainting using denoising diffusion probabilistic models. In *CVPR*, pages 11461–11471, 2022. 3

[23] Yongrui Ma, Shi Guo, Yutian Chen, Tianfan Xue, and Jin-wei Gu. Timelens-xl: Real-time event-based video frame interpolation with large motion. In *European Conference on Computer Vision*, pages 178–194. Springer, 2025. 2

[24] Anton Mitrokhin, Cornelia Fermüller, Chethan Parameshwara, and Yiannis Aloimonos. Event-based moving object detection and tracking. In *2018 IEEE/RSJ International Conference on Intelligent Robots and Systems (IROS)*, pages 1–9. IEEE, 2018. 3

[25] Anton Mitrokhin, Chengxi Ye, Cornelia Fermüller, Yiannis Aloimonos, and Tobi Delbrück. Ev-imo: Motion segmentation dataset and learning pipeline for event cameras. In *2019 IEEE/RSJ International Conference on Intelligent Robots and Systems (IROS)*, pages 6105–6112. IEEE, 2019. 3

[26] Yeongwoo Nam, Mohammad Mostafavi, Kuk-Jin Yoon, and Jonghyun Choi. Stereo depth from events cameras: Concentrate and focus on the future. In *Proceedings of the IEEE/CVF Conference on Computer Vision and Patter Recognition*, 2022. 4

[27] Chethan M Parameshwara, Nitin J Sanket, Chahat Deep Singh, Cornelia Fermüller, and Yiannis Aloimonos. 0-mms: Zero-shot multi-motion segmentation with a monocular event camera. In *2021 IEEE International Conference on Robotics and Automation (ICRA)*, pages 9594–9600. IEEE, 2021. 3

[28] Junheum Park, Chul Lee, and Chang-Su Kim. Asymmetric bilateral motion estimation for video frame interpolation. In *Proceedings of the IEEE/CVF international conference on computer vision*, pages 14539–14548, 2021. 3

[29] Adam Polyak, Amit Zohar, Andrew Brown, Andros Tjandra, Animesh Sinha, Ann Lee, Apoorv Vyas, Bowen Shi, Chih-Yao Ma, Ching-Yao Chuang, et al. Movie gen: A cast of media foundation models. *arXiv preprint arXiv:2410.13720*, 2024. 2

[30] Henri Rebecq, René Ranftl, Vladlen Koltun, and Davide Scaramuzza. High speed and high dynamic range video with an event camera. *IEEE transactions on pattern analysis and machine intelligence*, 43(6):1964–1980, 2019. 3

[31] Robin Rombach, Andreas Blattmann, Dominik Lorenz, Patrick Esser, and Björn Ommer. High-resolution image synthesis with latent diffusion models. In *CVPR*, 2022. 3

[32] Nataniel Ruiz, Yuanzhen Li, Varun Jampani, Yael Pritch, Michael Rubinstein, and Kfir Aberman. Dreambooth: Fine tuning text-to-image diffusion models for subject-driven generation. In *Proceedings of the IEEE/CVF conference on computer vision and pattern recognition*, pages 22500–22510, 2023. 3

[33] Christoph Schuhmann, Richard Vencu, Romain Beaumont, Robert Kaczmarczyk, Clayton Mullis, Aarush Katta, Theo Coombes, Jenia Jitsev, and Aran Komatsuzaki. Laion-400m: Open dataset of clip-filtered 400 million image-text pairs. *arXiv preprint arXiv:2111.02114*, 2021. 3

[34] Yang Song, Jascha Sohl-Dickstein, Diederik P Kingma, Abhishek Kumar, Stefano Ermon, and Ben Poole. Score-based generative modeling through stochastic differential equations. In *ICLR*, 2021. 3

[35] Timo Stoffregen, Cedric Scheerlinck, Davide Scaramuzza, Tom Drummond, Nick Barnes, Lindsay Kleeman, and Robert Mahony. Reducing the sim-to-real gap for event cameras. In *Computer Vision–ECCV 2020: 16th European Conference, Glasgow, UK, August 23–28, 2020, Proceedings, Part XXVII 16*, pages 534–549. Springer, 2020. 2, 6

[36] Lei Sun, Christos Sakaridis, Jingyun Liang, Peng Sun, Jiezhang Cao, Kai Zhang, Qi Jiang, Kaiwei Wang, and Luc Van Gool. Event-based frame interpolation with ad-hoc

deblurring. In *Proceedings of the IEEE/CVF Conference on Computer Vision and Pattern Recognition*, pages 18043–18052, 2023. [2](#), [3](#)

[37] Stepan Tulyakov, Daniel Gehrig, Stamatios Georgoulis, Julius Erbach, Mathias Gehrig, Yuanyou Li, and Davide Scaramuzza. Time lens: Event-based video frame interpolation. In *Proceedings of the IEEE/CVF conference on computer vision and pattern recognition*, pages 16155–16164, 2021. [6](#)

[38] Stepan Tulyakov, Alfredo Bochicchio, Daniel Gehrig, Stamatios Georgoulis, Yuanyou Li, and Davide Scaramuzza. Time lens++: Event-based frame interpolation with parametric non-linear flow and multi-scale fusion. In *Proceedings of the IEEE/CVF Conference on Computer Vision and Pattern Recognition*, pages 17755–17764, 2022. [2](#), [3](#)

[39] Zhou Wang, Alan C Bovik, Hamid R Sheikh, and Eero P Simoncelli. Image quality assessment: from error visibility to structural similarity. *IEEE transactions on image processing*, 13(4):600–612, 2004. [6](#)

[40] Lvmin Zhang, Anyi Rao, and Maneesh Agrawala. Adding conditional control to text-to-image diffusion models. In *ICCV*, 2023. [2](#), [3](#), [4](#)

[41] Richard Zhang, Phillip Isola, Alexei A Efros, Eli Shechtman, and Oliver Wang. The unreasonable effectiveness of deep features as a perceptual metric. In *Proceedings of the IEEE conference on computer vision and pattern recognition*, pages 586–595, 2018. [6](#)

[42] Xiang Zhang and Lei Yu. Unifying motion deblurring and frame interpolation with events. In *Proceedings of the IEEE/CVF Conference on Computer Vision and Pattern Recognition*, pages 17765–17774, 2022. [2](#), [3](#)

[43] Yuang Zhang, Jiaxi Gu, Li-Wen Wang, Han Wang, Junqi Cheng, Yuefeng Zhu, and Fangyuan Zou. Mimicmotion: High-quality human motion video generation with confidence-aware pose guidance. *arXiv preprint arXiv:2406.19680*, 2024. [3](#)

[44] Alex Zihao Zhu, Liangzhe Yuan, Kenneth Chaney, and Kostas Daniilidis. Ev-flownet: Self-supervised optical flow estimation for event-based cameras. *arXiv preprint arXiv:1802.06898*, 2018. [3](#)

[45] Alex Zihao Zhu, Liangzhe Yuan, Kenneth Chaney, and Kostas Daniilidis. Unsupervised event-based learning of optical flow, depth, and egomotion. In *Proceedings of the IEEE/CVF Conference on Computer Vision and Pattern Recognition*, pages 989–997, 2019. [3](#)